ADVANCED FUNCTIONAL MATERIALS

Efficient Isolation and Solubilization of Pristine Single-Walled Nanotubes in Bile Salt Micelles**

By *Wim Wenseleers*,* *Igor I. Vlasov*, *Etienne Goovaerts*, *Elena D. Obraztsova*, *Anatolii S. Lobach*, and *August Bouwen*

We have investigated a wide variety of surfactants for their efficiency in dissolving isolated single-walled carbon nanotubes (SWNTs) in water. In doing so, we have completely avoided the harsh chemical or mechanical conditions, such as acid or ultrasonic treatments, that are known to damage SWNTs. Bile salts in particular are found to be exceptionally effective in dissolving individual tubes, as evidenced by highly resolved optical absorption spectra, bright bandgap fluorescence, and the unprecedented resolution (~ 2.5 cm^{-1}) of the radial breathing modes in Raman spectra. This is attributed to the formation of very regular and stable micelles around the nanotubes providing an unusually homogeneous environment. Quantitative information concerning the degree of solubilization is obtained from absorption spectroscopy.

1. Introduction

Single-walled carbon nanotubes are very promising materials for a wide range of applications due to their unique mechanical, electronic, and optical properties.[1–5] However, their practical application has been hampered by their very low solubility, which is crucial to their processing.[6] In particular, as-produced nanotubes consist of many different diameters and chiralities—each with very different properties—and contain impurities (graphite, metal catalyst particles, etc.), and virtually all purification and separation methods for SWNTs that are currently being explored require the tubes to be processed as a liquid dispersion. The solubility of SWNTs can be enhanced by chemical substitution,[7] but this generates defect sites that perturb the electronic properties.[8] Therefore, SWNTs are usually dispersed using surfactants. However, in the vast majority of studies only one of the most common detergents (sodium dodecyl sulfate, SDS) is used, and surprisingly little research has been reported on the optimization of the surfactants. Polymers such as polyvinylpyrrolidone (PVP),[9] selected poly(phenylene-vinylene)s,[10,11] and DNA,[12,13] have also been found to act as useful surfactants for dispersing nanotubes. Last year, Islam et al. demonstrated that sodium dodecylbenzene sulfonate (DDBS) is significantly more effective than SDS in dispersing SWNTs,[14] and a transmission electron microscopy (TEM) study of the morphology of surfactants on carbon nanotubes has been reported.[15] Moore et al. have recently reported a comparison of a larger number of surfactants, and confirmed the relative superiority of DDBS, also including evidence from the increased resolution in absorption spectra.[16] Indeed, it is important to distinguish between true solubilization of individual nanotubes and the dispersion of bundles of tubes. O'Connell et al. have demonstrated that bundles and individual tubes can be separated by using centrifugation and that the pure individually dissolved nanotubes are fluorescent and display more resolved absorption bands.[17] In all solubilization methods reported to date though, use of (often very powerful) ultrasonic agitation and/or harsh chemical treatments is necessary, both of which are known to damage and cut SWNTs into short pieces.[6] In this work, we compare a wide range of surfactants for solubilization of SWNTs without exposure to such harsh conditions, and characterize the solubilization by absorption, fluorescence, and Raman spectroscopy in parallel.

[*] Dr. W. Wenseleers, Prof. E. Goovaerts, Prof. A. Bouwen
Physics Department, University of Antwerp
campus Drie Eiken
Universiteitsplein 1, B-2610 Antwerpen (Belgium)
E-mail: Wim.Wenseleers@ua.ac.be
Dr. I. I. Vlasov, Dr. E. D. Obraztsova
General Physics Institute
38 Vavilovstr., 119991 Moscow (Russia)
Dr. A. S. Lobach
Institute of Chemical Physics Problems, RAS
Chernogolovka, 142432 (Russia)

[**] The authors gratefully acknowledge L. Moens and S. Dewilde for the use of and kind assistance with the ultracentrifuge, U. Dettlaff-Weglikowska for the purification of HiPco SWNTs, and Ph. Lambin and F. Stellacci for stimulating discussions. W. W. is a Postdoctoral Fellow of the Fund for Scientific Research Flanders (Belgium) (FWO — Vlaanderen). Financial support from FWO in the group project G.0041.01 is gratefully acknowledged.

2. Results and Discussion

In order to provide an efficient solubilization, the surfactant i) should form very stable micelle structures around the SWNTs, as the dissolution of SWNTs competes with very strong aggregation forces due to the efficient π-stacking of the tubes, and ii) should posses a polar tail, preferably long and disordered, to provide a large solvatation shell to keep the long and rigid tubes suspended. If this polar tail is charged, aggregation is further prevented by the Coulombic repulsion between surfactant coated SWNTs. Although best results may therefore be expected for ionic surfactants, we also included a range of zwitterionic and non-ionic surfactants in our study (see Fig. 1), as different applications and separation methods (e.g., electro-

 DOI: 10.1002/adfm.200400130

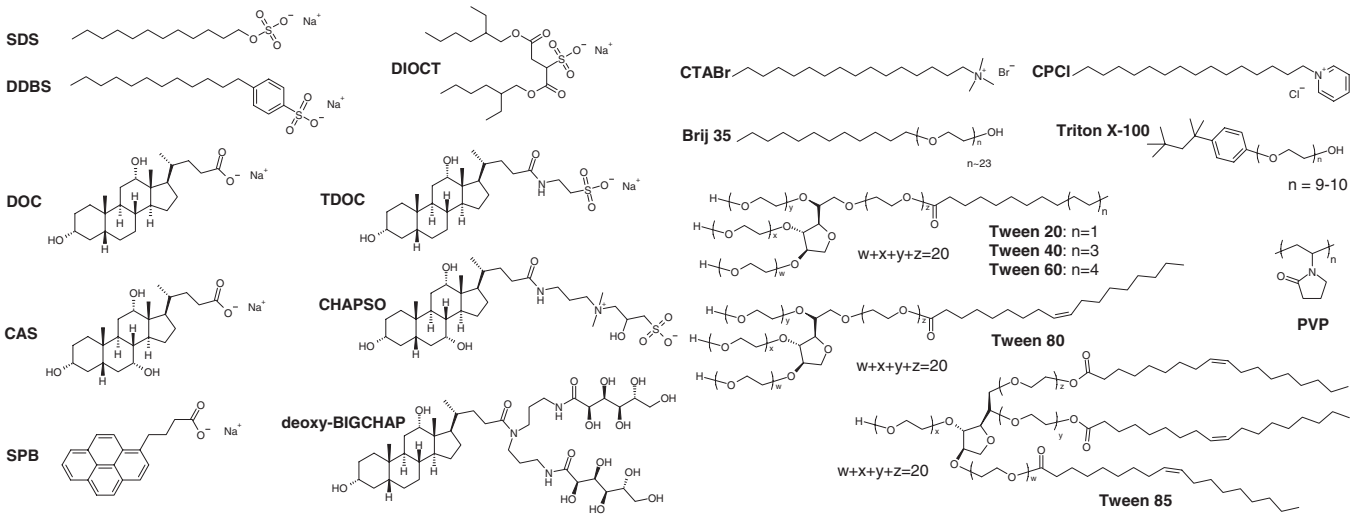

Figure 1. Chemical structures of the surfactants used in this study. Abbreviations: SDS: sodium dodecylsulfate, DDBS: sodium dodecylbenzenesulfonate, DIOCT: dioctyl sulfosuccinate, sodium salt, SPB: sodium pyrenebutyrate, CAS: sodium cholate, DOC: sodium deoxycholate, TDOC: sodium taurodeoxycholate, CTABr: cetyltrimethylammonium bromide, CPCl: cetylpyridinium chloride, PVP: polyvinylpyrrolidone.

phoresis and related techniques) have different requirements with respect to the charge state and chemical compatibility of the surfactant. In this study, we used SWNTs produced by the carbon arc method using a Ni/Y_2O_3 (1:1 ratio) catalyst.[18] These tubes are less pure (estimated ~20 %) than those produced by the high pressure CO (HiPco) method, but have a far narrower diameter distribution ($d = (1.46 \pm 0.15)$ nm, as determined from optical absorption data[19]), which largely simplifies their spectroscopic properties. On the other hand, at these relatively large diameters, neighboring types of nanotubes are very closely spaced so that the individual chiralities usually cannot be resolved spectroscopically. Surfactants were dissolved in water (or D_2O, for increased density in centrifugation and increased IR transparency in optical spectroscopy) at a concentration of 1 % wt./vol., and then added to the raw SWNT material. Solutions were very gently stirred for 3 days and then allowed to settle for another 3 days in order to sediment undissolved aggregates.

For a first screening, a relatively small amount of SWNT material (0.36 $g\,L^{-1}$) was dispersed into each surfactant solution in water. The settled solutions were characterized via absorption spectroscopy. This shows the typical SWNT absorption bands corresponding to transitions (hereafter referred to as "van Hove transitions") between the first, second, and third pairs of van Hove singularities in the density of states of semiconducting tubes (the third band overlapping with the first van Hove transition of metallic tubes),[20] superimposed on a broad background which closely follows an inverse proportionality with wavelength λ. A first evaluation of the different surfactants was obtained by comparing the amplitude of the first or second van Hove transitions (after background subtraction, see Sec. 4.2.) as a measure of SWNT concentration. For the more promising surfactants, we repeated the same procedure using higher concentrations (2, 10 $g\,L^{-1}$). The results are shown in Figure 2.

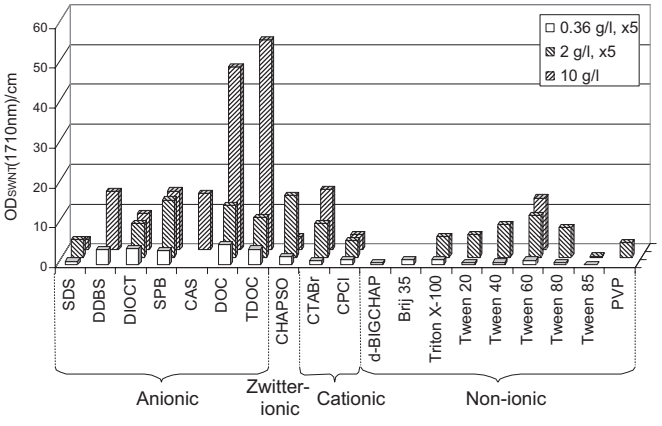

Figure 2. Peak SWNT absorbances (first van Hove transition at ~1710 nm) as a measure of relative SWNT concentration, for each surfactant and for different initial concentrations of the raw material, after settling for 3 days. Data for the lower two concentrations are magnified 5 times for clarity. For these two data series, the SWNT material was obtained from a common ethanol stock dispersion, while for the higher concentration data the as-produced raw material was used directly (see Sec. 4.1.).

Among the synthetic anionic surfactants, sodium dioctyl sulfosuccinate (DIOCT), which has a branched hydrophobic moiety, is far more efficient than the more traditional linear surfactant SDS. As reported recently, DDBS is also very efficient in dispersing the nanotubes, but has considerable disadvantages: for example, DDBS is not available in pure form, and the impurities present are believed to be important to the detergent properties of DDBS[21] (similar effects have been observed for SDS[22]). Also, the presence of an aromatic ring in this detergent limits its use in spectroscopic investigations. Even much higher nanotube absorbances are achieved with the natural bile salt detergents, especially the sodium salts of deoxycholic acid (DOC) and its taurine substituted analogue taurodeoxycholic

ADVANCED FUNCTIONAL MATERIALS

acid (TDOC). In fact, in the case of TDOC we have no indication that saturation was achieved, even after further increasing the amount of raw SWNT material to 20 g L^{-1}. It is also worth noting that these bile salts (especially DOC) have an excellent optical transparency, well into the UV (down to ~ 200 nm).

Among the cationic surfactants, CTABr also yields useful SWNT concentrations. CPCl is less efficient, and the first van Hove transition of the SWNT is strongly blue shifted by ~ 35 nm compared to most other surfactants suggesting a specific interaction of the pyridinium ring with the SWNTs. This implies that at least some of the CPCl molecules are inverted with the charged group pointing inward, which may explain the less efficient nanotube solubilization. Specific (π-stacking) interactions with aromatic rings have also been suggested to be responsible for the relatively high efficiency of DDBS and Triton X-100.[14] However, we did not observe a significant spectral shift for these surfactants (within an experimental error of ~ 5 nm), and efficient π–π interactions seem in fact unlikely for these two surfactants due to the steric hindrance of the bulky substituents (sulfonate and branched octyl respectively). Moreover, in DDBS, the aromatic ring is at the polar end of the molecule.

Non-ionic detergents lack the advantage of Coulomb repulsion to keep the SWNT containing micelles from aggregating. Therefore, the main factor determining the water solubility, in this case, is the presence of long and/or branched disordered polar chains—typically poly(ethylene glycol) chains. This results in the general trend, also observed by Moore et al.,[16] of increasing efficiency with increasing molecular weight of the surfactant. This is most clearly illustrated by the analogous series Tween 20, Tween 40, Tween 60, which differ only in the length of the alkyl chain. In strong contrast with other reported observations,[16] we, however, find that Tween 60 is the most efficient non-ionic surfactant, with Tween 80 being less efficient and Tween 85 yielding no significant SWNT solubilization (in [16], within the Tween series, a significant solubilization was obtained only for Tween 85). The latter two series differ in that they have one double bond forming a kink in their apolar chains, and Tween 85 has a completely different structure with three apolar chains and only one free standing polar branch, drastically reducing its water solubility (it is in fact designed for forming inverse micelles in apolar media). The bent apolar chains make molecular packing more difficult, probably resulting in less stable micelle structures. Not coincidentally, Tween 60, having the longest saturated chain and thus allowing a more regular packing, is also the only detergent of the Tween series which is solid at room temperature. Given the high efficiency of the bile salts, it seemed logical to consider non-ionic analogues of these as well. Unfortunately, although the zwitterionic cholesterol derivative CHAPSO still provides a significant SWNT solubilization, the non-ionic derivative deoxy-BIGCHAP yielded no useful SWNT concentrations. Clearly, the two saccharide tails are insufficient to provide the required water solubility.

Finally, instead of only relying on non-specific (hydrophobic) interactions to form stable micelle structures around the SWNTs, we also considered the use of specific (π-stacking) interactions to form an even more stable SWNT/surfactant complex. SWNTs are well known to bind to aromatic ring systems such as pyrene.[23,24] The anionic pyrene derivative SPB is indeed quite efficient in solubilizing SWNTs. This surfactant is very analogous to the cationic derivative used by Nakashima et al.,[25] but SPB (at basic pH) is at least two orders of magnitude more soluble in water, which probably also translates into improved surfactant properties. The π-stacking interaction with the pyrene groups perturbs the electronic properties of the SWNTs (as evidenced by a red shift of the first SWNT absorption bands by ~ 15 nm). This may be an undesirable complication when the spectroscopic analysis of the SWNTs themselves is envisaged, but the strong surfactant/SWNT interaction can also be very useful, for instance to improve the mechanical properties of polymer/SWNT composites[26] through a more efficient load transfer between polymer matrix and SWNTs, while avoiding covalent functionalization, which creates defect sites on the SWNTs and would thereby compromise the intrinsic strength of the tubes. To date, attempts to exploit the extraordinary mechanical strength of carbon nanotubes in reinforced polymer/nanotube composites have been largely limited by this poor load transfer, due to both a limited interfacial area, as many tubes remain aggregated in bundles, and the weakness of the polymer/nanotube interfacial interaction itself.[26]

Note that overall, the differences in solubility obtained with different surfactants in our study are larger than in previous studies.[14,16] This may be attributed to the fact that in previous work, the combined effects of cutting and solubilization were observed. The cutting of SWNTs during ultrasonication is likely to be enhanced when SWNTs are aggregated or entangled (STM images of SWNTs from sonicated dispersions also provide evidence for the fracture of entire bundles[27]), and therefore it is possible that the shortening of SWNTs occurs to a larger extent in inefficient surfactants, thus partially compensating for the lower intrinsic solubilizing efficiency. By avoiding ultrasonication altogether in this study, the solubilization is studied separately from the cutting effects.

Besides the fact that many of the surfactants are more effective than SDS, the absorption spectra (see also Sec. 4.2., Fig. 7) also show that there is a wide variation of the relative amplitude of the SWNT absorption bands compared to the $1/\lambda$ background. This allows us to conclude that most of this background is not intrinsic to the SWNT absorption, but rather to absorption and/or scattering by impurities (metal catalyst particles or graphitic particles and possibly also to scattering by large aggregates of bundles), and that SDS appears to preferentially dissolve these impurities, while other surfactants show a preferential dissolution of SWNTs. This partial selectivity can be used in order to improve previously reported[28] surfactant-based purification methods.

The first evaluation based on the absorbance yields an overall measure of the total amount of SWNTs dispersed, including separate tubes as well as small bundles or aggregates. For some of the more promising surfactants, we therefore ultracentrifuged (UCF) the dispersions under the conditions as in reference [9] (in D_2O; 4 h at 122 000 g), in order to separate individ-

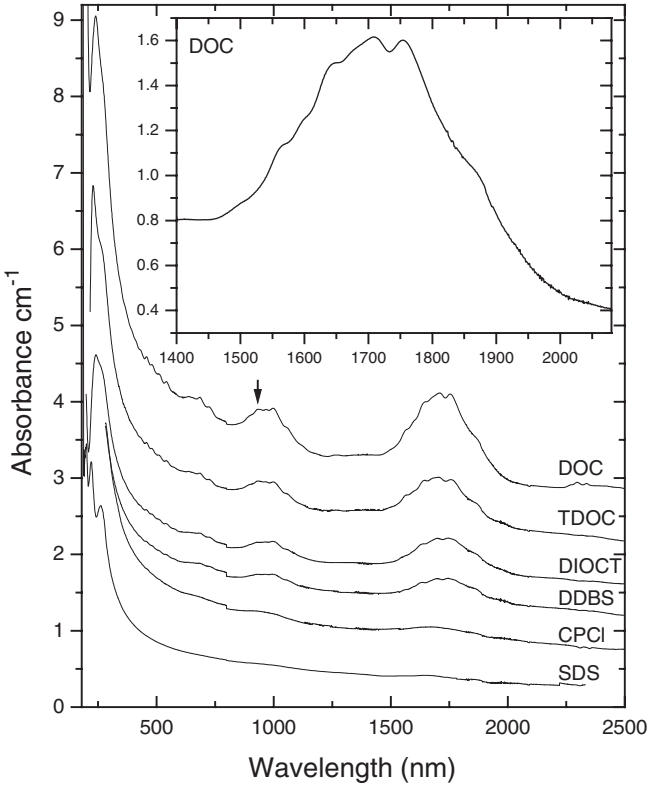

Figure 3. Absorption spectra of SWNT dispersions with different surfactants (starting from 10 mg raw material in 1 mL D_2O) after ultracentrifugation. No background subtraction (other than the baseline correction for solvent and surfactant absorption) was applied. Spectra are shifted vertically (steps of 0.5, starting from zero for SDS) for clarity. An arrow marks the excitation wavelength (930 nm) used for the fluorescence measurements of Figure 4.

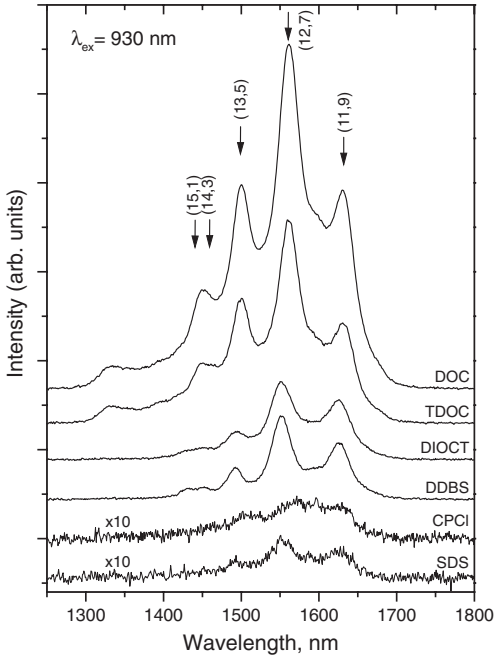

Figure 4. Fluorescence spectra, excited at 930 nm, of the same SWNT dispersions as in Figure 5.

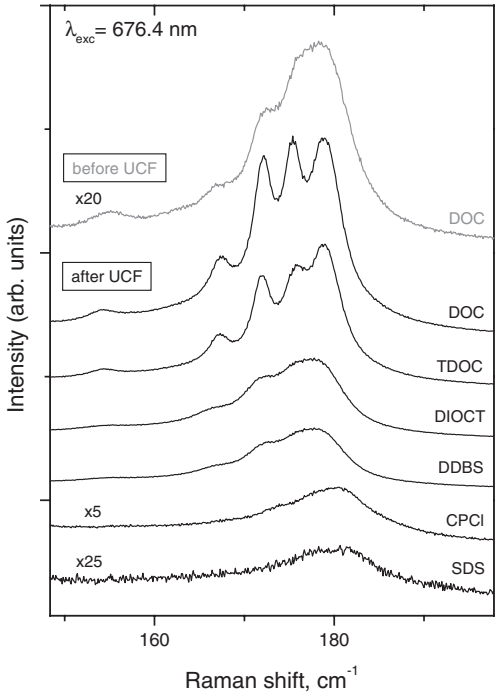

Figure 5. Radial breathing mode region of the Raman spectra, excited at 676.4 nm, for the same SWNT dispersions as in Figure 3, as well as for the SWNT/DOC solution before UCF. Spectra for CTABr and Tween 60 (not shown) were almost identical in shape to that for CPCl, but with higher intensities. The instrumental resolution was 0.34 cm^{-1}.

ually suspended tubes from bundles (very small bundles may still remain dispersed), and we investigated the suspensions (before and after UCF) by absorption, Raman and (after UCF) fluorescence spectroscopy. Results (after UCF) are shown in Figures 3–5.

By far the most interesting results were obtained with the natural bile salt detergents DOC and TDOC, which also showed the most efficient solubilization before centrifugation. Not only was the overall SWNT solubility strongly increased with these surfactants, as judged from the amplitude of the SWNT absorption bands, Raman intensity, and fluorescence intensity, but also the spectral resolution was improved dramatically, providing compelling evidence for an efficient solubilization of isolated nanotubes. For the first time, we obtained a clear sub-structure in the first van Hove transition of electric arc produced SWNTs. Arc-SWNTs have a relatively large average diameter (hence subsequent possible tube diameters are very closely spaced) and a very narrow diameter distribution, and in previous work the first van Hove transition was an essentially featureless band. Even in the very detailed analysis of the absorption spectrum of chemically solubilized arc-SWNTs by Lian et al.,[29] this band was well fitted with only two Gaussian components. In the present spectra in DOC or TDOC, we can observe about nine components in the first transition, as well as in the second transition (Lian et al. fitted the second band with only four components). The positions of the features

ADVANCED FUNCTIONAL MATERIALS

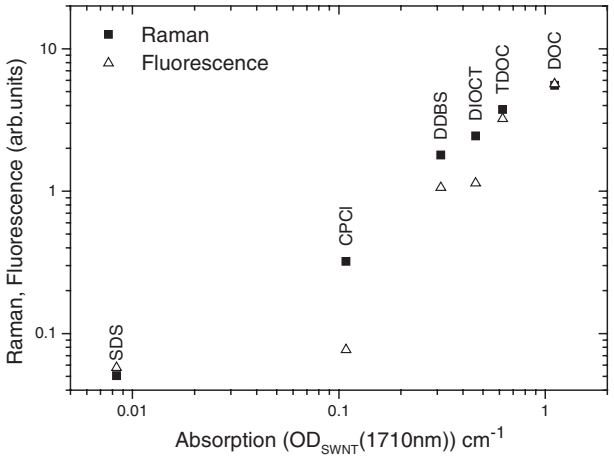

Figure 6. Correlation of integrated fluorescence and Raman intensities with absorbance for the ultracentrifuged SWNT solutions of Figures 3–5.

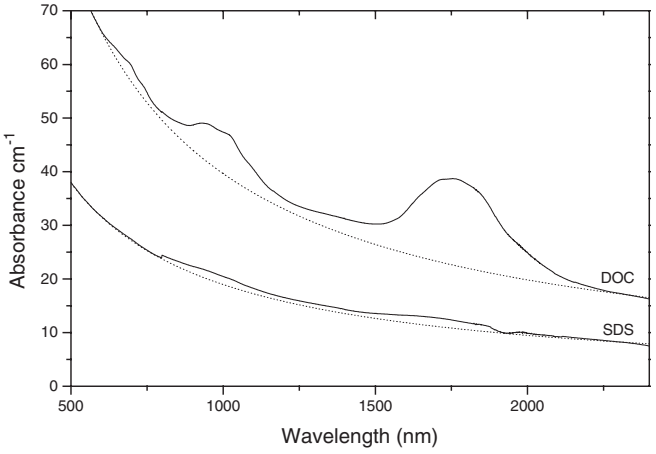

Figure 7. Absorption spectra of two SWNT solutions (using 10 g L^{-1} raw SWNT material) in D_2O with SDS and with DOC before ultracentrifugation. The $1/\lambda$ background to be subtracted is also shown (dotted lines) for each spectrum. The dip near 1900 nm is an artifact due to imperfect correction for the solvent absorption.

we observe are in fact in excellent agreement with positions of groups of nanotube types with similar transition energies extrapolated from the empirical relations derived by Weisman and co-workers from fluorescence emission/excitation data of HiPco tubes in SDS dispersion.[19,30] For instance, the pronounced absorption peak at ~ 933 nm corresponds to the series of semiconducting tubes (15,1), (14,3), (13,5), (12,7), (11,9), which all have closely spaced second transitions in the range 930–950 nm, but a wider spacing of their first van Hove transition energies. Indeed, when exciting into this narrow absorption feature, we observed strong discrete fluorescence peaks (see Fig. 4) close to the predicted bandgap for each of these five chiralities of SWNTs, from close to zig-zag to close to armchair. This is very different from the assignment of the less resolved absorption features by Lian et al. who assumed that only chiralities close to the armchair geometry occur in the arc-SWNTs.[29] The observed emission peaks also coincide with shoulders seen in the absorption spectrum (compare with Fig. 3, inset).

For the six surfactants studied by fluorescence spectroscopy, the SWNT fluorescence intensity scales roughly proportionally with the SWNT Raman intensity (after centrifugation) and the amplitude of the SWNT absorption bands (see Fig. 6). This suggests that the absorption and Raman measurements both provide a measure of SWNT concentration after centrifugation and that in most cases the fluorescence quantum efficiency does not depend strongly on the surfactant. Only CPCl appears to induce a strong (approximately seven-fold) reduction in fluorescence efficiency, and a noticeable drop in fluorescence efficiency is also observed for DDBS and DIOCT. Before centrifugation though, absorption spectroscopy is the technique of choice for estimating SWNT concentrations, because at high optical densities (due to both SWNTs and impurities) the varying penetration depth of the exciting light beam prevents (or at least complicates) quantitative intensity comparisons in Raman or fluorescence measurements. Besides using absorption as a relative measure of concentration, we also made a crude calibration relating the absorbance to actual SWNT concentrations based on measurements of nearly completely dissolved samples of purified HiPco SWNTs at low concentrations (see Sec. 4.2.). The results are (within the uncertainty on this crude calibration) consistent with an essentially complete dispersion of all the SWNTs present in the raw material with TDOC (after settling, but before UCF), up to the highest concentrations tested. For the TDOC solution (10 g L^{-1} raw SWNT material), the SWNT concentration was reduced from ~ 4.2 g L^{-1} to ~ 0.10 g L^{-1} upon UCF (i.e., 2.4 % of the dispersed tubes were retained). The fraction of dispersed tubes retained in the supernatant after UCF was comparable for DIOCT (5.1 %), DOC (2.4 %), CPCl (2.9 %), and DDBS (2.1 %), but much lower for SDS (0.3 %, of an already very low concentration of dispersed SWNTs: 0.20 g L^{-1} before and 0.67 mg L^{-1} after UCF), which is again consistent with SDS being less efficient at isolating SWNTs.

Also, in Raman spectra, a dramatically improved resolution of the radial breathing modes (RBMs) is obtained with DOC and TDOC (Fig. 5). As a result of the narrow diameter distribution, and the resulting efficient packing in bundles and strong coupling of RBMs of tubes in the bundles, RBM spectra of dispersions of arc-SWNT usually only show a single, almost featureless band. As the frequency shifts/splittings associated with this coupling of RBMs are theoretically predicted to be of the order of 15 cm^{-1}, with a large fraction of this occurring even for very small bundles,[31] it is important to fully separate bundles into individual tubes in order to achieve a significantly improved resolution in Raman spectra. For isolated HiPco-SWNTs in SDS micelles (possibly also containing small bundles) Strano et al.[32] recently deduced an improved RBM linewidth of ~ 11.5 cm^{-1} — to the best of our knowledge the narrowest linewidth previously reported in literature for SWNTs in liquid solution. In our TDOC and DOC solutions, the RBM modes are as narrow as ~ 2.5 cm^{-1} (FWHM), allowing to fully resolve the RBM modes of individual SWNT chiralities. This resolution is in fact higher than that obtained for individual SWNTs grown on Si/SiO_2 substrates by chemical vapor deposi-

tion,[33,34] for HiPco SWNTs,[35] laser and arc SWNTs,[36] even at low temperature, for which natural linewidths in the range 3–10 cm^{-1} were estimated (linewidths increasing with increasing diameter[34]). A higher resolution has been achieved only for the RBM of the inner tubes of double wall nanotubes, in which the outer wall is believed to provide an unusually unperturbed environment (but at the expense of a dramatic increase in complexity of the spectra).[37] Thus our observations prove that DOC and TDOC efficiently form solutions of individually separated SWNTs and that the cholesterol groups form very stable and homogeneous micelle structures around the SWNTs. Note that a fine structure of the RBM band is already noticeable in the Raman spectrum taken before UCF (upper curve in Fig. 5), which suggests that a significant fraction of the tubes (at least ~20 %) are dispersed in isolated form. Nevertheless, only ~2.5 % of the dispersed (individual plus bundled) tubes are left after UCF, the rest being lost either because many tubes are isolated over most of their length but still attached to or entangled in larger aggregates, or simply because long individual tubes are sedimented as well.

It is quite remarkable that the bile salts, which have been optimized by nature as detergents aiding in the emulsification and digestion of fats, also outperform all of the studied synthetic detergents in the solubilization of carbon nanotubes. In order to identify the structural features that make these bile salts so efficient we consider the general aspects important to the solubilization process. Thermodynamically, dissolved SWNTs in bile salt micelles will be stable if the Gibbs' free energy ($G = H - TS$) of this system is minimal. Unlike conjugated polymers (as well as smaller aromatic molecules such as the pyrene derivatives), in which the SWNT separation and solubilization process is governed by the very large π–π interaction energies,[38,39] the SWNT–surfactant interactions involved in the case of traditional detergents and bile salts are only very weak hydrophobic/hydrophilic van der Waals' interactions. However, in contrast with the more traditional detergents which have a linear and very flexible apolar tail, the more apolar half of the bile salts consists of a semi-rigid cholesterol group which usually (e.g., in the derivatives considered here) possesses both a hydrophobic and a hydrophilic face, depending on the number and substitution pattern of the hydroxy groups.[40] The flattened bean shape of this group is particularly suitable for stacking into ordered layers, hence the interaction energy between neighboring surfactant molecules is at least as important as the surfactant–SWNT interaction. The rigidity of the cholesterol group also reduces the entropic penalty associated with the organization into an ordered layer. In contrast, the conjugated polymers used to dissolve SWNTs provide a large interaction energy, but are forced into a particular conformation upon binding to the SWNTs.[39] The strong tendency of cholesterol derivatives to organize into ordered layers is exemplified by the fact that cholesterol is also a well-known building block for many chiral (= "cholesteric") liquid crystals.[41] Also, the monohydroxy substituted bile salt sodium lithocholate, a less polar and therefore less water soluble[40,42] analogue of DOC, was recently shown to form large and remarkably monodisperse nanotubular structures.[43] It is therefore not surprising that a very stable and ordered cylindrical layer is also easily formed around SWNT templates.

Besides the thermodynamic equilibrium condition, kinetic aspects are important to the solubilization process. In this sense, the smaller surfactant molecules such as the bile salts have a definite advantage over long chain polymers as dispersants. It is quite conceivable that in a system where both solute and dispersant are very long, entanglement (e.g., wrapping of polymer around SWNT bundles) can be a limiting factor to the dissolution kinetics. In contrast, the small bile salt molecules can diffuse rapidly and quickly cover SWNT surfaces as soon as they become exposed (either thermally or by mechanical agitation). As these molecules combine into a well-packed shell the aggregation of the SWNTs is effectively prevented.

Despite giving significant SWNT concentrations, some surfactants yield a broad unresolved RBM spectrum, even after UCF. Possibly these surfactants solubilize both individual tubes and entire bundles. Such a loss of selectivity is plausible for the non-ionic surfactants since they require extremely long chains to achieve a useful solubilization (e.g., Tween 60, PVP). However, also for individually dissolved SWNTs a broadening of the RBM peaks may be induced, if the surfactant micelle structure is more disordered.

3. Conclusions

Bile salt detergents are extremely efficient in solubilizing pristine individual SWNTs, and their micelles form an unusually unperturbed environment, opening new possibilities for spectroscopic investigations of nanotubes in liquid solutions as well as for their processing and purification. As these surfactants are strongly chiral, they even offer the prospect — at least in principle — to distinguish left- and right-handed chiral tubes of the same diameter and chiral angle.

4. Experimental

4.1. Materials and Procedures

Surfactants were obtained from Acros [dodecyl sulfate, sodium salt 99 % (SDS); dodecylbenzenesulfonic acid, sodium salt, 88 % (DDBS); deoxycholic acid, sodium salt 99 % (DOC); taurodeoxycholic acid, sodium salt, hydrate, 97 % (TDOC); cholic acid, sodium salt 99 % (CAS); cetyltrimethylammonium bromide, 99+ % (CTABr); cetylpyridinium chloride monohydrate, 96+ % (CPCl); Triton X-100; Brij 35; Tween 20; Tween 40; Tween 60; Tween 80; Tween 85; poly(vinylpyrrolidone), average molecular weight, M_w 58 000, K29-32 (PVP)], Aldrich [dioctyl sulfosuccinate, sodium salt 99 % (DIOCT)] or AppliChem [CHAPSO, +98 %; deoxy-BIGCHAP, +95 % (d-BIGCHAP)], and used as received. Sodium pyrenebutyrate (SPB) was obtained from the free acid (1-pyrenebutyric acid, 99 %, Acros) by addition of an excess of NaOH (pH ~ 12.5). A stoichiometric amount of NaOH (pH ~ 8.7) was not sufficient to obtain a significant SWNT solubilization with SPB. We also checked that with other surfactants a high pH did not improve SWNT solubilization.

Surfactants were dissolved in water (or D_2O, for increased density in centrifugation and increased IR transparency for optical spectroscopy) at a concentration of 1 % wt./vol. and then added to the raw SWNT material. Solutions were very gently stirred (8 mm × 3 mm stirring bar

in 4 mL vial, ~200 rpm) for 3 days and then allowed to settle for another 3 days to sediment undissolved aggregates (a ~10 min centrifugation at 3000 g gave similar results, and a longer settling time of 1–2 weeks did not change results significantly either, suggesting that the dispersions were close to equilibrium after 3 days). For a first screening, 1 mg of SWNT material was dispersed in 2.75 mL of surfactant solution in H_2O.

Because there might be a significant variation in the composition of subsequent 1 mg samples of the SWNT material (even though taken from the same batch), we also repeated the procedure using SWNT samples obtained by distributing and drying a single stock dispersion of SWNTs in ethanol, but this confirmed the same relative trends among the surfactants—except that (for all surfactants) the compacted pellets obtained from the dried ethanol dispersions were in general more difficult to dissolve than the raw SWNT material. The latter is similar to previous observations that nanotubes can spontaneously rearrange into thicker ropes upon purification [44]. Results shown in Figure 2 for the 0.36 g L^{-1} and 2 g L^{-1} solution were obtained using this procedure, while for the 10 g L^{-1} data the raw material was dissolved directly into the surfactant solution. This may explain why the latter gives a more than five-fold increase in absorbance in several cases. Peak positions of the first absorption band of the SWNTs were compared for settled solutions (not ultracentrifuged) obtained using SWNT material from a common ethanol dispersion. With few exceptions (CPCl, SPB, as discussed in Sec. 3.), within an experimental error of ~5–10 nm, no significant variation of this peak position was found. Moore et al. recently demonstrated that the smaller variations occurring with non-specifically interacting surfactants can still be detected with great precision in fluorescence [16].

In all experiments a surfactant concentration of 1% wt./vol. was used. This concentration was not optimized, but in many cases this is more than the critical micelle concentration, so generally we do not expect dramatic improvements with higher surfactant concentrations. For SDS, this concentration of 1% wt./vol. is close to optimal [45]. At the very highest SWNT concentrations obtained with the more efficient surfactants however, the SWNT concentration (in wt./vol. %) becomes comparable to the surfactant concentration, and therefore the ratio of surfactant concentration to SWNT concentration may start to become the limiting factor.

Raman spectra were recorded in a backscattering geometry using a Dilor XY triple spectrometer with liquid nitrogen cooled CCD detection, and a Kr^+ ion laser (Spectra-Physics model 2020) for excitation. Spectra were corrected for the spectral/spatial sensitivity variation of the spectrometer/detector based on the fluorescence from known dyes. Laser powers incident on the sample were ~40 mW for the ultracentrifuged solutions. For high concentration solutions before UCF, lower powers were used as appropriate to prevent local heating of the samples. The spectrometer was used in high dispersion mode with 1800 lines mm^{-1} gratings and an entrance slit width of 50 μm (spectral resolution = 0.34 cm^{-1}).

Fluorescence spectra were recorded using a Jobin-Yvon H250 monochromator (600 lines/mm^{-1} grating, 1 μm blaze) with a Peltier-cooled InGaAs PIN detector (EG&G, HTE-2642) and lock-in amplifier. The incident beam from a Ti:sapphire laser (Spectra-Physics model 3900S) was modulated at 113 Hz using a chopper. Fluorescence spectra were not corrected for the spectral sensitivity of the detector, which is roughly flat up to ~1630 nm and drops to ~10 % of its peak sensitivity at 1700 nm.

UCF was performed using a Kontron Centrikon T-1080 ultracentrifuge with swing-out rotor (TST 28) and 1.3 mL polyallomer tubes. After UCF (4 h at 122 000 g, 20 °C) the central ~1 mL of the supernatant was transferred in a separate vial for further measurements.

Absorption spectra were recorded using a Varian Cary 5E UV-VIS-IR spectrometer, using quartz cells with path lengths in the range of 1 to 10 mm and scaled to a common path length of 10 mm. For the highest concentration solutions before UCF, absorbances were too high to be measured directly in a 1 mm cell, and two alternative methods were used instead. Firstly, absorption spectra were obtained by 20- to 40-fold dilution (of the supernatant after sedimentation) with surfactant solution, just before the absorption measurement, and scaled accordingly. Secondly, measurements were performed directly on the undiluted solutions in capillary cells (pathlength = 5–50 μm), internally calibrating the pathlength based on the D_2O absorption bands. Absorbances obtained with both methods were in good agreement, but with larger random errors (~20 %) on the measurements in capillary cells (attributed to inhomogeneous cell thickness). The 10 g L^{-1} data represented in Figure 2 are those obtained by dilution.

4.2. Estimation of SWNT Concentrations from Absorption Spectra

Relative Concentrations: The absorption spectra were first used in order to estimate the relative SWNT concentrations. For the solutions before UCF, in which the characteristic van Hove bands are superimposed onto a very strong background (see Fig. 7), an appropriate background subtraction scheme was needed in order to obtain a reliable measurement of the SWNT absorbance OD_{SWNT}. First, a $1/\lambda$ background was subtracted, setting the absorbance at $\lambda = 584$ nm (a wavelength outside the main SWNT absorption bands) to zero. This removes the major component of the background. As this background subtraction (as well as the instrumental baseline) is not perfect, we then used an additional linear background subtraction in the narrow range of the first SWNT band. For the measurements reported in this paper, we thus derived the peak absorbance at ~1710 nm corresponding to the first van Hove transition of the semiconducting tubes (or an average of absorbance over a narrow range around these wavelengths) as a measure of relative SWNT concentration. We also checked that measuring the amplitude of the second van Hove transition (at ~972 nm) confirms the same relative trends. In all cases (even with SPB and CPCl), surfactant dependence of the SWNT band positions was small enough that it had a negligible effect on the peak absorbance measurements.

Estimate of Absolute Concentrations: Finally, we also roughly related the measured absorbance to the actual SWNT concentration. To this end, we prepared solutions of purified HiPco SWNTs (~99 %) at known concentrations in the range of 0.005–0.11 g L^{-1} (in D_2O with 1 % DOC), following the same procedure as for the arc-tubes, except that we also used ultrasonication to approach 100 % dissolution of the tubes. The HiPco tubes were obtained commercially from Carbon Nanotechnologies (Houston TX, USA), and purified by U. Dettlaff-Weglikowska (Max-Planck Institute, Stuttgart, Germany) as described in reference [35]. The dispersions were not perfectly stable (some sedimentation—albeit possibly due to impurities—was noticeable after a few days), but the absorbance scaled linearly with added concentration of SWNT material, indicating that dissolution was close to complete. In order to be able to compare the absorbances of the HiPco tubes with those of the arc-SWNTs, which have a different diameter distribution, we assumed that the oscillator strength of the lowest energy absorption band scales with the total nanotube length (in line with the theoretical scaling of the joint density of states with length [46]), in other words, with the ratio mass/diameter. After subtraction of a $1/\lambda$ background (setting $OD(472\text{ nm}) = 0$), the first and second van Hove transitions, plotted on an energy scale, were approximated as two Gaussian bands. The first band (centered at 0.945 eV with a width of 0.288 eV), normalized to a concentration of 1 g L^{-1} and a pathlength of 1 cm, was found to possess an integrated (over energy) absorbance of 3.0 eV. Taking into account that only ~2/3 of the tubes are semiconducting, this integral corresponds to an oscillator strength of 1.9×10^{-3} per carbon atom, for the first absorption band of the semiconducting tubes. Accounting for the different average diameters for the HiPco (~0.96 nm) and arc-SWNTs (~1.46 nm), hence a 1.52 times lower integrated absorption per mass for the arc-SWNTs, this corresponds to the following calibration factor for the arc-SWNTs:

$$C[\text{g L}^{-1}] = 0.08 \times OD_{\text{SWNT}}\,(1710\text{ nm}) \quad (1)$$

where we used a conversion factor from integrated to peak absorbance (for these arc-SWNTs) derived from a high quality absorption spectrum of a high SWNT concentration solution (with DOC) after UCF.

Given the many uncertainties, (for instance, the background subtraction probably overcorrects (i.e., underestimates) the absorbance when applied to the very broad absorption spectra of the HiPco tubes, hence underestimating the oscillator strength and overestimating the above calibration factor and concentrations) this currently only represents an approximate order of magnitude estimate. Thus, for the highest SWNT concentration solution in Figure 2 (10 g L^{-1} raw material, with TDOC), this estimate yields a SWNT concentration of ~ 4.2 g L^{-1} (before UCF), suggesting that all the SWNTs present in the raw material were dissolved — in agreement with the conclusion that saturation was not yet reached (20 g L^{-1} raw material gave OD_{SWNT}(1710 nm) ~ 130, hence a SWNT concentration of ~ 10 g L^{-1}). For consistency, the same background subtraction scheme was also used when estimating SWNT concentrations after UCF, even though the background was very small in this case.

Received: March 26, 2004
Final version: June 18, 2004

[1] R. H. Baughman, A. A. Zakhidov, W. A. de Heer, *Science* **2002**, *297*, 787.
[2] M. Terrones, *Annu. Rev. Mater. Res.* **2003**, *33*, 419.
[3] S. B. Sinnott, R. Andrews, *Crit. Rev. Solid State Mater. Sci.* **2001**, *26*, 145.
[4] Special issue on Carbon Nanotubes, *Acc. Chem. Res.* **2002**, *35*, 997.
[5] S. Reich, C. Thomsen, J. Maultzsch, *Carbon Nanotubes — Basic Concepts and Physical Properties*, Wiley-VCH, Weinheim, Germany **2004**.
[6] J. Hilding, E. A. Grulke, Z. G. Zhang, F. Lockwood, *J. Dispersion Sci. Technol.* **2003**, *24*, 1.
[7] A. Hirsch, *Angew. Chem. Int. Ed.* **2002**, *41*, 1853.
[8] D. Tasis, N. Tagmatarchis, V. Georgakilas, M. Prato, *Chem. Eur. J.* **2003**, *9*, 4001.
[9] M. J. O'Connell, P. Boul, L. M. Ericson, C. Huffman, Y. H. Wang, E. Haroz, C. Kuper, J. Tour, K. D. Ausman, R. E. Smalley, *Chem. Phys. Lett.* **2001**, *342*, 265.
[10] S. Curran, A. P. Davey, J. Coleman, A. Dalton, B. McCarthy, S. Maier, A. Drury, D. Gray, M. Brennan, K. Ryder, M. L. de la Chapelle, C. Journet, P. Bernier, H. J. Byrne, D. Carroll, P. M. Ajayan, S. Lefrant, W. Blau, *Synth. Met.* **1999**, *103*, 2559.
[11] H. S. Woo, R. Czerw, S. Webster, D. L. Carroll, J. Ballato, A. E. Strevens, D. O'Brien, W. J. Blau, *Appl. Phys. Lett.* **2000**, *77*, 1393.
[12] M. Zheng, A. Jagota, E. D. Semke, B. A. Diner, R. S. McLean, S. R. Lustig, R. E. Richardson, N. G. Tassi, *Nat. Mater.* **2003**, *2*, 338.
[13] J. N. Barisci, M. Tahhan, G. G. Wallace, S. Badaire, T. Vaugien, M. Maugey, P. Poulin, *Adv. Funct. Mater.* **2004**, *14*, 133.
[14] M. F. Islam, E. Rojas, D. M. Bergey, A. T. Johnson, A. G. Yodh, *Nano Lett.* **2003**, *3*, 269.
[15] C. Richard, F. Balavoine, P. Schultz, T. W. Ebbesen, C. Mioskowski, *Science* **2003**, *300*, 775.
[16] V. C. Moore, M. S. Strano, E. H. Haroz, R. H. Hauge, R. E. Smalley, J. Schmidt, Y. Talmon, *Nano Lett.* **2003**, *3*, 1379.
[17] M. J. O'Connell, S. M. Bachilo, C. B. Huffman, V. C. Moore, M. S. Strano, E. H. Haroz, K. L. Rialon, P. J. Boul, W. H. Noon, C. Kittrell, J. P. Ma, R. H. Hauge, R. B. Weisman, R. E. Smalley, *Science* **2002**, *297*, 593.
[18] E. D. Obraztsova, J. M. Bonard, V. L. Kuznetsov, V. I. Zaikovskii, S. M. Pimenov, A. S. Pozarov, S. V. Terekhov, V. I. Konov, A. N. Obraztsov, A. P. Volkov, *Nanostruct. Mater.* **1999**, *12*, 567.
[19] S. M. Bachilo, M. S. Strano, C. Kittrell, R. H. Hauge, R. E. Smalley, R. B. Weisman, *Science* **2002**, *298*, 2361.
[20] H. Kataura, Y. Kumazawa, Y. Maniwa, I. Umezu, S. Suzuki, Y. Ohtsuka, Y. Achiba, *Synth. Met.* **1999**, *103*, 2555.
[21] K. D. Danov, S. D. Kralchevska, P. A. Kralchevsky, G. Broze, A. Mehreteab, *Langmuir* **2003**, *19*, 5019.
[22] P. A. Kralchevsky, K. D. Danov, V. L. Kolev, G. Broze, A. Mehreteab, *Langmuir* **2003**, *19*, 5004.
[23] R. J. Chen, Y. G. Zhang, D. W. Wang, H. J. Dai, *J. Am. Chem. Soc.* **2001**, *123*, 3838.
[24] S. G. Stepanian, V. A. Karachevtsev, A. Y. Glamazda, U. Dettlaff-Weglikowska, L. Adamowicz, *Mol. Phys.* **2003**, *101*, 2609.
[25] N. Nakashima, Y. Tomonari, H. Murakami, *Chem. Lett.* **2002**, 638.
[26] M. Cadek, J. N. Coleman, K. P. Ryan, V. Nicolosi, G. Bister, A. Fonseca, J. B. Nagy, K. Szostak, F. Beguin, W. J. Blau, *Nano Lett.* **2004**, *4*, 353.
[27] L. P. Biró, S. Lazarescu, P. Lambin, P. A. Thiry, A. Fonseca, J. B. Nagy, A. A. Lucas, *Phys. Rev. B* **1997**, *56*, 12 490.
[28] J. M. Bonard, T. Stora, J. P. Salvetat, F. Maier, T. Stockli, C. Duschl, L. Forro, W. A. deHeer, A. Chatelain, *Adv. Mater.* **1997**, *9*, 827.
[29] Y. F. Lian, Y. Maeda, T. Wakahara, T. Akasaka, S. Kazaoui, N. Minami, N. Choi, H. Tokumoto, *J. Phys. Chem. B* **2003**, *107*, 12 082.
[30] R. B. Weisman, S. M. Bachilo, *Nano Lett.* **2003**, *3*, 1235.
[31] L. Henrard, V. N. Popov, A. Rubio, *Phys. Rev. B* **2001**, *64*, 205 403.
[32] M. S. Strano, S. K. Doorn, E. H. Haroz, C. Kittrell, R. H. Hauge, R. E. Smalley, *Nano Lett.* **2003**, *3*, 1091.
[33] A. Jorio, R. Saito, J. H. Hafner, C. M. Lieber, M. Hunter, T. McClure, G. Dresselhaus, M. S. Dresselhaus, *Phys. Rev. Lett.* **2001**, *86*, 1118.
[34] A. Jorio, C. Fantini, M. S. S. Dantas, M. A. Pimenta, A. G. Souza, G. G. Samsonidze, V. W. Brar, G. Dresselhaus, M. S. Dresselhaus, A. K. Swan, M. S. Unlu, B. B. Goldberg, R. Saito, *Phys. Rev. B* **2002**, *66*, 115 411.
[35] V. A. Karachevtsev, A. Y. Glamazda, U. Dettlaff-Weglikowska, V. S. Kurnosov, E. D. Obraztsova, A. V. Peschanskii, V. V. Eremenko, S. Roth, *Carbon* **2003**, *41*, 1567.
[36] M. N. Iliev, A. P. Litvinchuk, S. Arepalli, P. Nikolaev, C. D. Scott, *Chem. Phys. Lett.* **2000**, *316*, 217.
[37] R. Pfeiffer, H. Kuzmany, C. Kramberger, C. Schaman, T. Pichler, H. Kataura, Y. Achiba, J. Kurti, V. Zolyomi, *Phys. Rev. Lett.* **2003**, *90*, 225 501.
[38] A. B. Dalton, C. Stephan, J. N. Coleman, B. McCarthy, P. M. Ajayan, S. Lefrant, P. Bernier, W. J. Blau, H. J. Byrne, *J. Phys. Chem. B* **2000**, *104*, 10 012.
[39] M. I. H. Panhuis, A. Maiti, A. B. Dalton, A. van den Noort, J. N. Coleman, B. McCarthy, W. J. Blau, *J. Phys. Chem. B* **2003**, *107*, 478.
[40] A. Roda, A. F. Hofmann, K. J. Mysels, *J. Biol. Chem.* **1983**, *258*, 6362.
[41] *Handbook of Liquid Crystal Research* (Eds: P. J. Collings, J. S. Patel), Oxford University Press, New York **1997**.
[42] C. O. Mills, P. Milkiewicz, D. P. Molloy, D. J. Baxter, E. Elias, *Biochim. Biophys. Acta* **1997**, *1336*, 485.
[43] P. Terech, A. de Geyer, B. Struth, Y. Talmon, *Adv. Mater.* **2002**, *14*, 495.
[44] K. B. Shelimov, R. O. Esenaliev, A. G. Rinzler, C. B. Huffman, R. E. Smalley, *Chem. Phys. Lett.* **1998**, *282*, 429.
[45] B. Vigolo, A. Penicaud, C. Coulon, C. Sauder, R. Pailler, C. Journet, P. Bernier, P. Poulin, *Science* **2000**, *290*, 1331.
[46] P. Lambin, *C. R. Phys.* **2003**, *4*, 1009.

